Enhanced Wide-Spectrum Vibration Suppression Based on Adaptive Loop Shaping

Liting Sun, Xu Chen and Masayoshi Tomizuka

(CML Report)

Department of Mechanical Engineering
UC Berkeley

December 2015

Abstract

In linear feedback control, the attenuation of disturbances at the designer-selected frequencies is subjected to the fundamental limitation of undesired error amplifications at other frequencies, due to the "waterbed" effect that is induced from Bode's Integral Theorem. In the presence of unknown disturbances with high-frequency wide-spectrum peaks, such undesired error amplifications severely degrades the closed-loop servo performance, and are extremely difficult to control using traditional loop shaping techniques. In this paper, a direct adaptive control approach is proposed based on adaptive loop shaping and disturbance observer (DOB). The proposed algorithm offers more flexibilities in controlling the "waterbed" effect, to achieve enhanced attenuation of the unknown wide-spectrum disturbances. Verification of the proposed algorithm is provided by simulations of hard disk drives (HDDs) for audio vibration suppression.

The work has been submitted to The 2016 American Control Conference, July 6–8, Boston, MA, USA.

Contents

1 Introduction

Precision motion systems such as hard disk drives (HDDs), commonly encounter various external disturbances that must be suppressed to achieve the highest positioning accuracy and best servo performance. According to the frequency characteristics, the external disturbances can be categorized into two different groups: 1) narrow-band disturbances where the energy of the signals are highly concentrated at several known or unknown frequencies, as shown in Fig. 1(a), and 2) wide-spectrum disturbances whose spectral peaks are much wider, as shown in Fig. 1(b). Moreover, the frequency characteristics of such disturbances can be time-varying and/or environment/product-dependent. The spectral peaks also might occur at frequencies beyond the open loop servo bandwidth [1, 2]. For example, for the audio vibrations in modern HDDs, both the center frequencies and the widths of spectral peaks change in different operation environments and in different products; and the spectral peaks can appear at frequencies greater than 1000Hz [3]. Such disturbances with wide spectral peaks at high frequencies are difficult to suppress by traditional feedback control, due to the well-known "waterbed" effect [4]. As the system uncertainties become large at high frequencies, error amplifications that accompany the suppression of high-frequency diturbances will deteriorate the robustness of the closed loop and even cause system instability.

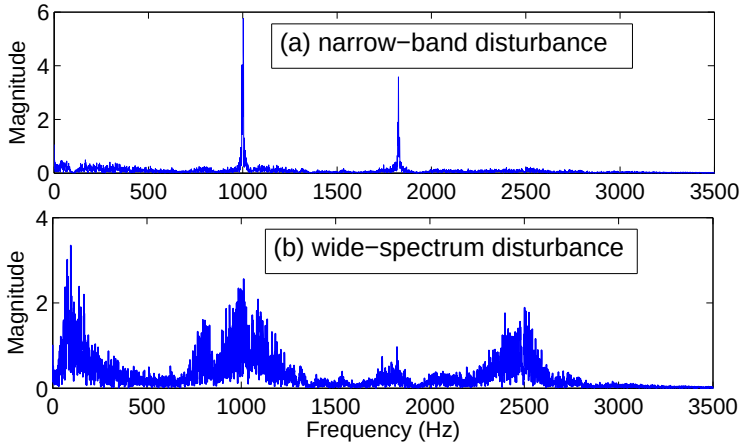

Figure 1: Examples of different disturbance signals

The attenuation of such band-shaped vibrations have attracted great attention of researchers. For the narrow-band case, extensive algorithms such as the peak filter [5, 6], Youla-parameterized compensator [7, 8, 9], adaptive notch filter [10, 11], and narrow-band disturbance observer (DOB) [12, 13, 14] have been developed and achieved good performance. Based on the internal model principle (IMP) [15], these works adaptively generate deep but narrow notches in the closed-loop sensitivity functions at the frequencies where the disturbances dominates, therefore the closed loops are shaped "locally" without bringing significant influences to other frequencies. In the presence of wide-spectrum vibrations, however, it is difficult to tune for the optimal notch widths in these algorithms. A narrow notch cannot provide sufficient attenuation to the wide-spectrum disturbances; yet a wide notch will bring large error amplifications at other frequencies and hence compromises the achievable performance. To address this problem, Chen et. al proposed to place a group of pre-designed poles and zeros [16] in the Q filter design and an offline optimization-based design approach is derived in [17]. Sun et. al [18] developed an adaptive DOB with a lattice-form IIR (Infinite Impulse Response) notch filter, which can automatically tune the width of the notch filter online for an optimal overall performance.

In this paper, a direct adaptive controller based on adaptive loop shaping and DOB is proposed. By introducing more adaptation freedom in the Q filter, this approach offers more flexibilities in controlling the "waterbed" effect. Attenuation of disturbances at the designer-selected frequencies are achieved with reduced error amplifications at other critical frequencies. Therefore, the overall performance for disturbance attenuation is enhanced. Verification is given in Section 5 by simulation results of a benchmark problem in HDDs for wide-spectrum audio vibration suppression.

2 Controller Structure

Figure 2 shows the controller structure with DOB for disturbance suppression in a regulation problem. $P(z^{-1})$ is the sampled plant and $C(z^{-1})$ is an existing feedback controller that stabilizes the system and provides a baseline servo performance. m, $P_n(z^{-1})$ and $P_{an}(z^{-1})$, respectively, represent the relative degree of $P(z^{-1})$, its nominal model and the delay-free nominal model, i.e., $z^{-m}P_{an}(z^{-1})$=$P_n(z^{-1})$≈$P(z^{-1})$. Therefore, $P_{an}^{-1}(z^{-1})$ is causal. To make $P_{an}^{-1}(z^{-1})$ stable, stable inverse techniques such as Zero-Phase-Error (ZPE)

inverse [19] can be used if the plant is non-minimum phase. $Q(z^{-1})$ is the Q filter to be designed to offer loop shaping ability and robustness. The signals $d(k)$, $e(k)$, $u(k)$, $y(k)$ and $n(k)$ are, respectively, the lumped input disturbance signal, the position error signal (PES), the control signal, the output signal and the measurement noise in the system.

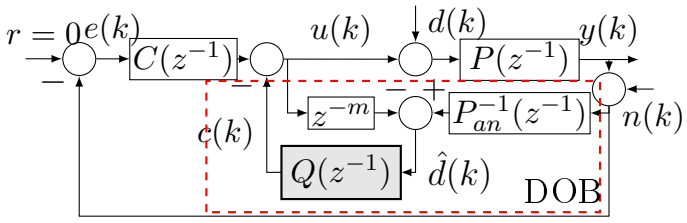

Figure 2: Block diagram of the controller structure with DOB

From Fig. 2, it is derived that $\hat{d}(k)$ is a contaminated and delayed estimate of $d(k)$, given by

$$\begin{aligned}\hat{d}(k) &= P_{an}^{-1}(q^{-1})\left\{P(q^{-1})\left[u(k)+d(k)\right]+n(k)\right\}-q^{-m}u(k)\\ &\approx d(k-m)+P_{an}^{-1}(q^{-1})n(k),\end{aligned} \tag{1}$$

where q^{-1} denotes the one-step delay operator in time domain. Therefore, to construct a compensation signal $c(k)$ that cancels out $d(k)$, i.e., $c(k)\approx d(k)$, $Q(z^{-1})$ needs to offer 1) m-step phase compensation and 2) frequency filtering ability that can maximally recover $d(k)$ from the noise-contaminated $\hat{d}(k)$. To see the role of $Q(z^{-1})$ from the loop-shaping perspective, the sensitivity function $S(z^{-1})$ (i.e., the output disturbance-rejection function) in Fig. 2 is computed as

$$S=\frac{1-z^{-m}Q}{1+PC+Q\left(PP_{an}^{-1}-z^{-m}\right)}. \tag{2}$$

Recalling $z^{-m}P_{an}(z^{-1})\approx P(z^{-1})$, $S(z^{-1})$ is simplified to

$$S\approx\left(1-z^{-m}Q\right)/\left(1+PC\right)=\left(1-z^{-m}Q\right)S_0,$$

where $S_0=1/\left(1+PC\right)$ is the baseline sensitivity function corresponding to the baseline controller $C(z^{-1})$. As a small $S(z^{-1})$ corresponds to strong attenuation of $d(k)$, the term $1-z^{-m}Q$ thus serves as an add-on frequency shaping term on top of $S_0(z^{-1})$, to enhance the performance of the controller for disturbance suppression. For example, letting $e^{-j\omega m}Q(e^{-j\omega})=1$ gives $S(e^{-j\omega})\approx 0$, i.e., perfect disturbance rejection at frequency ω.

To suppress the aforementioned band-shaped disturbances in Fig. 1, $1-z^{-m}Q(z^{-1})$ should introduce small gains at frequencies where the spectral peaks appear. Assume that f_0 is the center frequency of one peak, then based on IMP, $1-z^{-m}Q(z^{-1})$ should contain the internal model of $d(k)$, i.e., $1-2\cos\omega_0 z^{-1}+z^{-2}$ ($\omega_0=2\pi f_0$), so that $(1-q^{-m}Q(q^{-1}))\,d(k)\approx 0$. Therefore, we consider the following design

$$\begin{aligned} 1-z^{-m}Q(z^{-1}) &= \frac{A_N(1,z^{-1})}{A_N(\alpha,z^{-1})}J(z^{-1}) \\ Q(z^{-1}) &= \frac{B_Q(z^{-1})}{A_N(\alpha,z^{-1})} \end{aligned} \tag{3}$$

where $A_N(1,z^{-1})/A_N(\alpha,z^{-1}) \triangleq N(z^{-1})$ is a lattice-form IIR notch filter, with $A_N(\gamma,z^{-1})=1-(1+\gamma)\cos\omega_0 z^{-1}+\gamma z^{-2}$, $\gamma=\{1,\alpha\}$. This special notch filter $N(z^{-1})$ provides 1) a notch at frequency f_0 and 2) symmetric gains w.r.t f_0 [18, 20]. If there are multiple spectral peaks in $d(k)$, for example, n peaks at frequencies $f_i (i=1,\cdots,n)$, $A_N(\gamma,z^{-1})$ can be extended to

$$A_N(\gamma,z^{-1})=\prod_{i=1}^{n}\left(1-(1+\gamma)\cos\omega_i z^{-1}+\gamma z^{-2}\right), \omega_i=2\pi f_i,$$

with $\gamma=\{1,\alpha\}$. The design parameter $\alpha\in(0,1)$ controls the notch widths of $N(z^{-1})$ at f_i and the magnitude of $N(z^{-1})$ at other frequencies. As α approaches 1, the approximate notch width $NW=2\arctan\frac{1-\alpha}{1+\alpha}$ becomes small and the DC/Nyquist-gain $2/(1+\alpha)$ gets close to 1, namely, $A_N(1,z^{-1})/A_N(\alpha,z^{-1})$ approximates a perfect notch filter.

Recalling (2), the shape of $N(z^{-1})$ and $J(z^{-1})$ on the right-hand side of (3) will be directly reflected in the new sensitivity function $S(z^{-1})$. Multiplying $A_N(\alpha,z^{-1})$ to both sides of (3), we have

$$A_N(\alpha,z^{-1})=z^{-m}B_Q(z^{-1})+A_N(1,z^{-1})J(z^{-1}), \tag{4}$$

which is a Diophantine equation. Given z^{-m}, $A_N(1,z^{-1})$, and $A_N(\alpha,z^{-1})$, the unknown $B_Q(z^{-1})$ and $J(z^{-1})$ can be solved by matching the coefficients of z^{-i}. The minimum-order solution of (4) gives the desired Q filter in (3) if

$$\begin{cases} \deg\left(A_N(\alpha,z^{-1})\right) \le m+\deg\left(B_Q(z^{-1})\right) \\ \deg\left(B_Q(z^{-1})\right)+m=\deg\left(J(z^{-1})\right)+\deg\left(A_N(1,z^{-1})\right)=\deg\left(A_N(\alpha,z^{-1})\right)+m-1 \end{cases}$$

is satisfied. Such minimum-order solution, however, offers no freedom in designing the structure of $B_Q(z^{-1})$ since it is internally determined by the algebraic equation. The minimum-order $Q(z^{-1})$ can work well for the problem of narrow-band disturbance rejection, where $N(z^{-1})$ is a narrow notch filter with $|N(e^{-j\omega_0})| \approx 0$ and $|N(e^{-j\omega})| \approx 1, \omega \neq \omega_0$, so that little amplification is induced in $S(z^{-1})$ at other frequencies. As the notch width becomes wider for wide-spectrum disturbance rejection, $|N(e^{-j\omega})|$ at $\omega \neq \omega_0$ becomes larger and cannot be neglected anymore. Therefore, to adaptively control the "location" of the undesired gain amplifications, more design freedom to the term $J(z^{-1})$ should be introduced, which equivalently transforms into more design freedom in $B_Q(z^{-1})$ according to (4).

Thus, the new $B_Q(z^{-1})$ in the proposed algorithm is set as

$$B_Q(z^{-1}) = B_{Qm}(z^{-1}) B_{Qa}(z^{-1}) \tag{5}$$

where $B_{Qm}(z^{-1})$ represents a minimum-order polynomial in z-domain with $\deg(B_{Qm}(z^{-1})) = \deg(A_N(1, z^{-1})) - 1$; and $B_{Qa}(z^{-1})$ provides additional loop shaping freedom. The order of $B_Q(z^{-1})$ is denoted as r and should satisfy $r > \deg(A_N(1, z^{-1})) - 1$ for solving the Diophantine equation.

Figure 3 shows an example design of introducing more freedom in $B_Q(z^{-1})$. In Fig. 3, $B_{Qa}(z^{-1}) = 1 - z^{-1}$ provides small gains of $Q(z^{-1})$ at low frequencies, which, in the loop-shaping prospective, makes the low-frequency gains of $1 - z^{-m} Q(z^{-m})$ be close to 1, i.e., gain amplifications at low frequencies in $S(z^{-1})$ will be reduced compared to the minimum-order design (the dash-dotted curve).

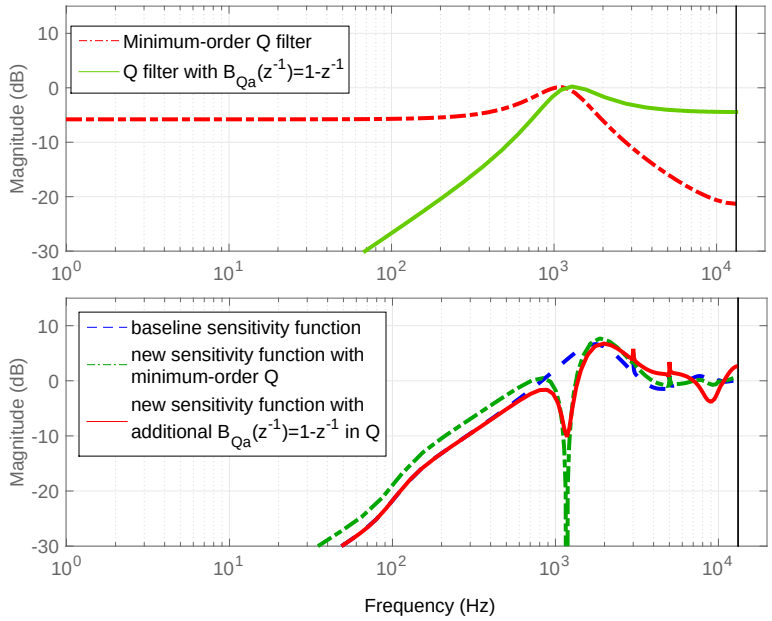

Figure 3: An example design of introducing additional loop shaping freedom in $B_Q(z^{-1})$

3 Direct Adaptive Loop Shaping for Wide - spectrum Vibration Suppression

As previously discussed, if the additional zeros in $B_Q(z^{-1})$ in (5) are predesigned offline, the control structure cannot effectively deal with disturbances with varying frequency characteristics. Therefore, the additional freedoms introduced in $B_Q(z^{-1})$ should adaptively shape the frequency characteristic of the add-on term $1-z^{-m}Q(z^{-1})$. By such adaptation in real time, disturbances at the spectrum-peak frequencies can be maximally attenuated and the error amplifications at other critical frequencies can be minimized. In this section, the adaptation of the proposed controller in Section 2 will be addressed.

3.1 Adaptive DOB structure with enhanced loop shaping

Figure 4 presents the proposed direct adaptive controller based on DOB and enhanced loop shaping. Here, the central Q filter is equipped with adaptable parameters in $B_Q(z^{-1})$. Recalling (5) and representing $B_Q(z^{-1})$ in a polynomial form, we get

$$\begin{aligned} B_Q(z^{-1}) &= B_{Qm}(z^{-1})B_{Qa}(z^{-1}) \\ &= b_0 + b_1 z^{-1} + b_2 z^{-2} + \cdots + b_r z^{-r}, \\ r &> \deg\left(A_N(1, z^{-1})\right) - 1. \end{aligned} \tag{6}$$

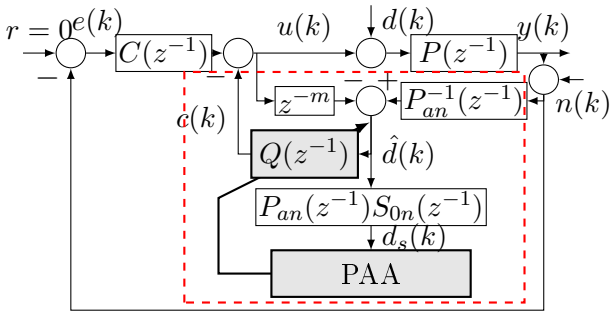

Figure 4: Block diagram of the proposed adaptive DOB structure with enhanced loop shaping

Similar to most regulation problems, our goal is to minimize $\|e(k)\|$ in the presence of the band-limited $d(k)$, particularly those with wide spectral peaks. Note that $\hat{d}(k)$ is a contaminated and delayed estimate of $d(k)$ as derived in (1), and that $z^{-m}P_{an}(z^{-1}) \approx P(z^{-1})$, $S(z^{-1}) \approx (1 - z^{-m}Q)\, S_0$. The output $e(k)$ can be expressed as (if $n(k)$ is small compared to $d(k)$)

$$\begin{aligned} e(k) &= -P(q^{-1})S(q^{-1})d(k) \\ &\approx -q^{-m}P_{an}(q^{-1})\left(1 - z^{-m}Q(z^{-1})\right) S_{0n}(q^{-1})d(k) \\ &= -\left(1 - z^{-m}Q(q^{-1})\right) P_{an}(q^{-1})S_{0n}(q^{-1})d(k-m) \\ &\approx -\left(1 - z^{-m}Q(q^{-1})\right) P_{an}(q^{-1})S_{0n}(q^{-1})\hat{d}(k) \\ &= -\left(1 - z^{-m}Q(q^{-1})\right) d_s(k), \end{aligned} \tag{7}$$

where $S_{0n}(q^{-1})$ is the nominal baseline sensitivity function given by

$$S_{0n}(q^{-1})=1/\left(1+P_n(q^{-1})C(q^{-1})\right).$$

$d_s(k)$ is the signal as shown in Fig. 4. Thus, minimizing $\|e(k)\|$ is equivalent to minimizing $\|(1-q^{-m}Q(q^{-1}))\,d_s(k)\|$ where the parameters of $B_Q(q^{-1})$ can then be updated online.

Remark 1: Practically, the effect of $n(k)$ will not cause severe problems to the adaptation and the convergence of the parameters. Most precision-motion systems have small gains at high frequencies where the noise usually dominates, namely, $|P_{an}(e^{-j\omega})|$ is small at high frequencies. Therefore, passing $\hat{d}(k)$ through $P_{an}(z^{-1})S_{0n}(z^{-1})$ will filter out $n(k)$.

3.2 Adaptation algorithm

As a direct adaptive control scheme, we need to define an *error equation* that reflects the difference between the optimal parameters of $B_Q(z^{-1})$ and the current ones [7]. Assume that at time index k, the updated $B_Q(z^{-1})$ is $\hat{B}_Q(k,z^{-1})$, then based on (3) and (7), the output signal $y(k+1)$ (in regulation problem, $y(k+1)=-e(k+1)$) in Fig. 4 is given by

$$y(k+1)=\left(1-q^{-m}\frac{\hat{B}_Q(k,q^{-1})}{A_N(\alpha,q^{-1})}\right)d_s(k+1). \tag{8}$$

Note that the relationship in (3) holds for both the current and the optimal $B_Q(z^{-1})$. Reordering terms and substituting (3) into (8), we obtain (the index q^{-1} is omitted here due to space limit)

$$\begin{aligned} y(k+1)&=\left(q^{-m}\frac{B_Q}{A_N(\alpha)}+\frac{A_N(1)}{A_N(\alpha)}J-q^{-m}\frac{\hat{B}_Q(k)}{A_N(\alpha)}\right)d_s(k+1)\\ &=\left(B_Q-\hat{B}_Q(k)\right)\frac{q^{-m}}{A_N(\alpha)}d_s(k+1)\\ &\quad+\frac{A_N(1)}{A_N(\alpha)}J\,d_s(k+1), \end{aligned} \tag{9}$$

where the signal $\frac{A_N(1,q^{-1})}{A_N(\alpha,q^{-1})}J(q^{-1})d_s(k+1)=v(k+1)$ will asymptotically converge towards zero since $\frac{A_N(1,q^{-1})}{A_N(\alpha,q^{-1})}J(q^{-1})$ is designed to include the internal

model of main components in $d_s(k)$ (i.e., the disturbance signal with spectrum peaks). Therefore, $y(k+1)$ can be used as the *a priori* error $\epsilon^0(k+1)$ for adaptation. Defining

$$\begin{aligned} w(k)&=\frac{q^{-m}}{A_N(\alpha,q^{-1})}d_s(k+1),\\ \theta&=[b_0,b_1,\cdots,b_r]^T,\\ \hat{\theta}(k)&=\left[\hat{b}_0(k),\hat{b}_1(k),\cdots,\hat{b}_r(k)\right]^T,\\ \Phi(k)&=[w(k),w(k-1),\cdots,w(k-r)]^T, \end{aligned} \tag{10}$$

and recalling (8), we can simplify the relationship between the *a priori* error $\epsilon^0(k+1)$ and the adaptive parameters $\hat{\theta}(k)$ to

$$\epsilon^0(k+1)=d_s(k+1)-\hat{\theta}^T(k)\Phi(k). \tag{11}$$

For the adaptation of $\hat{\theta}$, the Recursive-Least-Square (RLS) based parameter adaptation algorithm (PAA) is:

$$\hat{\theta}\,(k+1)=\hat{\theta}\,(k)+F(k)\Phi(k)\frac{\epsilon^0(k+1)}{1+\Phi^T(k)F(k)\Phi(k)} \tag{12}$$

$$\epsilon^0(k+1)=y(k+1) \tag{13}$$

$$F(k+1)=\frac{1}{\lambda(k+1)}\left\{F(k)-\frac{F(k)\Phi(k)\Phi^T(k)F(k)}{\lambda(k+1)+\Phi^T(k)F(k)\Phi(k)}\right\} \tag{14}$$

$$\lambda(k+1)=\lambda_{end}-[\lambda_{end}-\lambda(k)]\,\lambda_0 \tag{15}$$

in which the exponentially decreasing forgetting factor $\lambda(k)\in(0,1]$ in (15) is introduced to improve the convergence speed [21].

Remark 2: In the proposed algorithm, it is assumed that $A(\alpha,z^{-1})$ (the denominator of $Q(z^{-1})$) is designed based on prior knowledge on the center frequencies of the spectral peaks in $d(k)$ and remains fixed, namely, $A_N(\alpha,z^{-1})=1-(1+\alpha)\cos\omega_0 z^{-1}+\alpha z^{-2}$. Such configuration will guarantee the stability of $Q(z^{-1})$ during the adaptation. If no prior knowledge of the center frequencies is available, online frequency identification techniques such as [22, 13] can be employed first to estimate this information and then $Q(z^{-1})$ can be designed.

Remark 3: Actually, the direct adaptation of $B_Q(z^{-1})$ help relax the requirement for accurate center frequencies. The simulation results in Section

5 show that the proposed algorithm enhances the performance robustness in the presence of uncertainties in the center frequencies.

4 Stability analysis

4.1 Stability of the controller

This section discusses the stability of the proposed control scheme in Section 3. Based on previous discussion, we have

- The baseline controller $C(z^{-1})$ stabilizes the closed-loop system, i.e., all poles of $1/\left(1+P(z^{-1})C(z^{-1})\right)$ are stable;
- Within $\omega \in [0, 2\pi\times 2000]$, $P(e^{-j\omega})\approx e^{-j\omega}P_{an}(e^{-j\omega})$ holds, i.e., the mismatch between the plant and its nominal model is negligible;
- $Q(z^{-1})$ is stable for all possible $\hat{B}_Q(z^{-1})$ since its denominator $A_N(\alpha, z^{-1})$ remains stable;

Therefore, when $P(z^{-1})\approx z^{-m}P_{an}(z^{-1})$ satisfies, the structure in Fig. 4 is essentially a special Youla parameterization [23] and the stability is automatically guaranteed with stable Q filters. When $P(z^{-1})\neq z^{-m}P_{an}(z^{-1})$, namely, the plant model is subject to certain bounded uncertainty $\triangle(z^{-1})$ such that $P(z^{-1})=z^{-m}P_{an}(z^{-1})\left(1+\triangle\left(z^{-1}\right)\right)$, robust stability analysis will apply. Recalling (2), the closed-loop characteristic equation is reduced to

$$1+P(z^{-1})C(z^{-1})+Q(z^{-1})z^{-m}\triangle\left(z^{-1}\right)=0. \tag{16}$$

Therefore, the closed-loop system is stable in the presence of $\triangle(z^{-1})$ if

$$|Q(e^{-j\omega})|<\left|\frac{1+P(e^{-j\omega})C(e^{-j\omega})}{\triangle(e^{-j\omega})}\right|, \forall\omega. \tag{17}$$

4.2 Stability of the PAA and parameter convergence

Based on (9) and (10), the *a posteriori* error $\epsilon(k+1)$ of the adaptation algorithm is defined as

$$\epsilon(k+1)=\left(\theta^T-\hat{\theta}^T(k+1)\right)\Phi(k)+v(k+1). \tag{18}$$

The relationship between the *a posteriori* error and the *a priori* error is given by

$$\epsilon(k+1)=\frac{\epsilon^0(k+1)}{1+\Phi^T(k)F(k)\Phi(k)}. \tag{19}$$

Moreover, the PAA listed in (12)-(15) uses series-parallel-predictor structure [24], the stability (in the sense of Popov hyperstability) of which can be proved by constructing an equivalent feedback system with a strict positive real (SPR) linear feedforward block and a nonlinear feedback block that satisfies the Popov inequality [25]. The linear block is constant $(1-\max(\lambda(k))/2)>0$ in this case. The signal $v(k+1)$ in $\epsilon(k+1)$ (as shown in (18)) is a vanishing input signal in the equivalent feedback system and will not influence the stability of the adaptation process.

Therefore, the *a posterior* error asymptotically approaches 0, namely, $\lim_{k\to\infty}\epsilon(k+1)=0$ and $\lim_{k\to\infty}\left(\hat{\theta}^T(k+1)-\theta^T\right)\Phi(k)=0$. One can also remark that the signal $w(k+1)$ in (10) is bounded due to the bounded $d_s(k+1)$ and fixed $A(\alpha,z^{-1})$. The vector regressor $\Phi(k)$ is thus also bounded, which concludes $\lim_{k\to\infty}\epsilon^0(k+1)=\lim_{k\to\infty}\epsilon(k+1)\left(1+\Phi^T(k)F(k)\Phi(k)\right)=0$.

From the asymptotic convergence of $\epsilon(k+1)$, we also get

$$\lim_{k\to\infty}\left[\sum_{i=0}^{r}\left(b_i-\hat{b}_i(k+1)\right)q^{-i}\right]w(k-i)=0, \tag{20}$$

which means that either of the following two conditions is satisfied: (1) $\lim_{k\to\infty}\hat{b}_i(k)=b_i$, $i=0,1,\cdots r$ and (2) $\sum_{i=0}^{r}\left(b_i-\hat{b}_i(k+1)\right)q^{-i}$ includes all the modes of $w(k)$ (a filtered version of the disturbance $d(k)$ as defined in (10)). Recall that $r\geqslant\deg(A_N(\alpha,z^{-1}))=2n$ where n is the number of the spectral peaks in $d(k)$. For narrow-band disturbances as shown in Fig. 1(a), the order of the internal model of $d(k)$ is also $2n$. Therefore in such cases, the second condition might be true and as a result, the parameter convergence condition ($\lim_{k\to\infty}\hat{b}_i(k)=b_i$, $i=0,1,\cdots r$) cannot be guaranteed. In the case of wide-spectrum disturbances, however, the second condition is practically hard to satisfy. The wide-spectrum disturbances contain rich frequency components except for those at the spectrum-peak frequencies, namely, the order of the internal model of $d(k)$ is much greater than $\deg(A_N(\alpha,z^{-1}))$ (actually, additional structured zeros are provided by the optimal $J(z^{-1})$). Therefore, with proper selection of r, the only condition to satisfy (20) is

$\lim_{k\to\infty} \hat{b}_i(k)=b_i$, $i = 0, 1, \cdots r$, which means that the parameter convergence can be achieved.

5 Case Study

In this section, the proposed adaptive control scheme is applied to a HDD benchmark problem [26] for suppression of wide-spectrum audio vibrations.

5.1 Hard disk drive system

A single-stage HDD plant in track-following mode is used in this simulation. In such HDD systems, the read/write arm is actuated by a voice coil motor and the goal is to regulate the arm in the presence of various external vibrations. With a sampling frequency of F_s=26400Hz, Fig. 5 shows the frequency responses of the discrete-time full-order plant $P(z^{-1})$[1] and its nominal model $P_n(z^{-1})$. The relative degree of the plant is m=3 and $P(e^{-j\omega})\approx P_n(e^{-j\omega})$ holds for frequencies up to 2kHz. A PID controller $C(z^{-1})$ stabilizes the system and provides a baseline closed-loop servo performance with a bandwidth of about 800Hz. Beyond the servo bandwidth, the closed-loop system has limited performance for disturbance rejection with $|S_0(e^{-j\omega})|$ close to or greater than 1.

[1]Several notch filters have been incorporated into the plant for resonance attenuation.

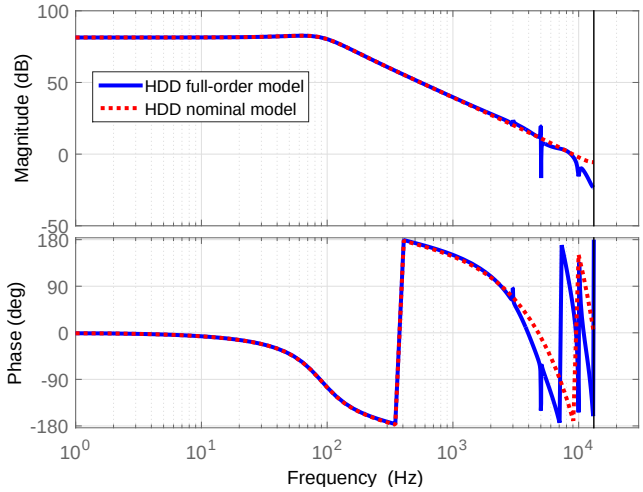

Figure 5: Frequency responses of the full-order plant and nominal model of the HDD

Audio vibration is a typical type of external disturbances that can severely influence the performance of the HDD. They mainly come from the audio systems in computers. As discussed in Section 1, the audio vibrations in HDD system often have varying wide-spectrum peaks, and the spectral peaks can appear beyond the servo bandwidth, as shown in Fig. 1.

5.2 Simulation results

Figure 6 shows the spectra of the PES, respectively, with the baseline controller (Fig. 6(a)), with the minimum-order Q filter for compensation (Fig. 6(b)) and with the proposed direct adaptive control for compensation (Fig. 6(c)). Both the minimum-order Q filter and the proposed controller can effectively attenuate the vibration at the peak frequency of about 1172Hz. The minimum-order Q filter, however, has brought larger error amplifications at low frequencies, as shown in Fig. 6(b) and Fig. 6(d). Such error amplifications compromised the control performance with 3σ=45.15% track. The proposed approach, on the other hand, has achieved better performance with 3σ=38.26% track. By introducing additional loop shaping freedom in $B_Q(z^{-1})$, it has adaptively "placed" the undesired error amplifications at other frequencies that will not cause significant increase of the error signal (Fig. 6(e)). Therefore, the overall position error is further reduced.

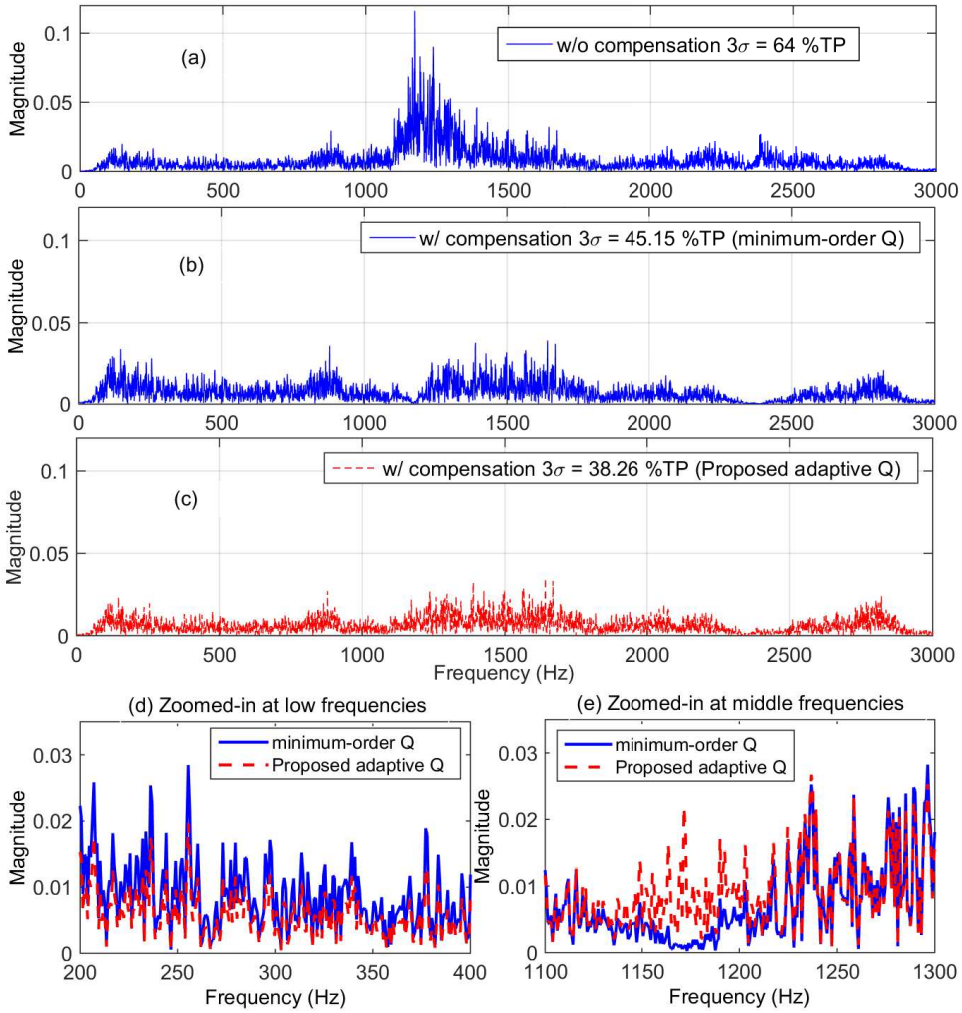

Figure 6: Frequency domain of PES w/ and w/o compensation

Figure 7 gives the frequency responses of the converged Q filter and the corresponding shaping term $1-z^{-m}Q(z^{-1})$. We can see that the shaping term with the proposed approach has much smaller gains (close to 1) at low frequencies, i.e., the good low-frequency-vibration-rejection ability of the baseline controller has been maximally preserved. Figure 7 also shows the evolution of the adaptive parameters (r=5, six parameters). Note that the convergence speed is fast. For example, if the disk is spinning at 7200rpm (revolution per minute), it only takes about 0.5 revolution (4×10^{-3}s) for the

parameters to converge.

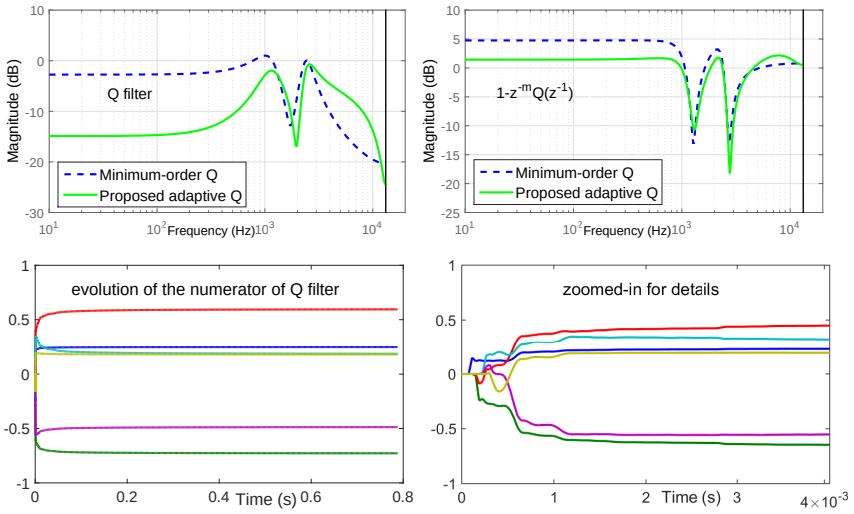

Figure 7: The Q filters and parameter convergence

As mentioned in Remark 3.2, the proposed approach allows uncertainties in the center frequencies of the vibration spectral peaks. Figure 8 shows the PES in time domain and in frequency domain, for the cases with the minimum-order Q filter and the proposed direct adaptive Q filter, respectively. With the actual center frequency at 1172Hz, the f_0 in $A(\gamma, z^{-1})$ in (3) has been set to be 900Hz. Such uncertainty significantly degrades the achievable performance of the minimum-order solution, which generates a wrong notch at 900Hz in the corresponding shaping term $1-z^{-m}Q(z^{-1})$. Thus, little attenuation to the actual disturbance at 1172Hz was achieved. The proposed approach, however, enhances the robustness of the local loop shaping technique with much better performance. The converged shaping term $1-z^{-m}Q(z^{-1})$ offers a more accurate notch at 1140Hz and therefore the spectral peak of the vibration in PES has been effectively suppressed.

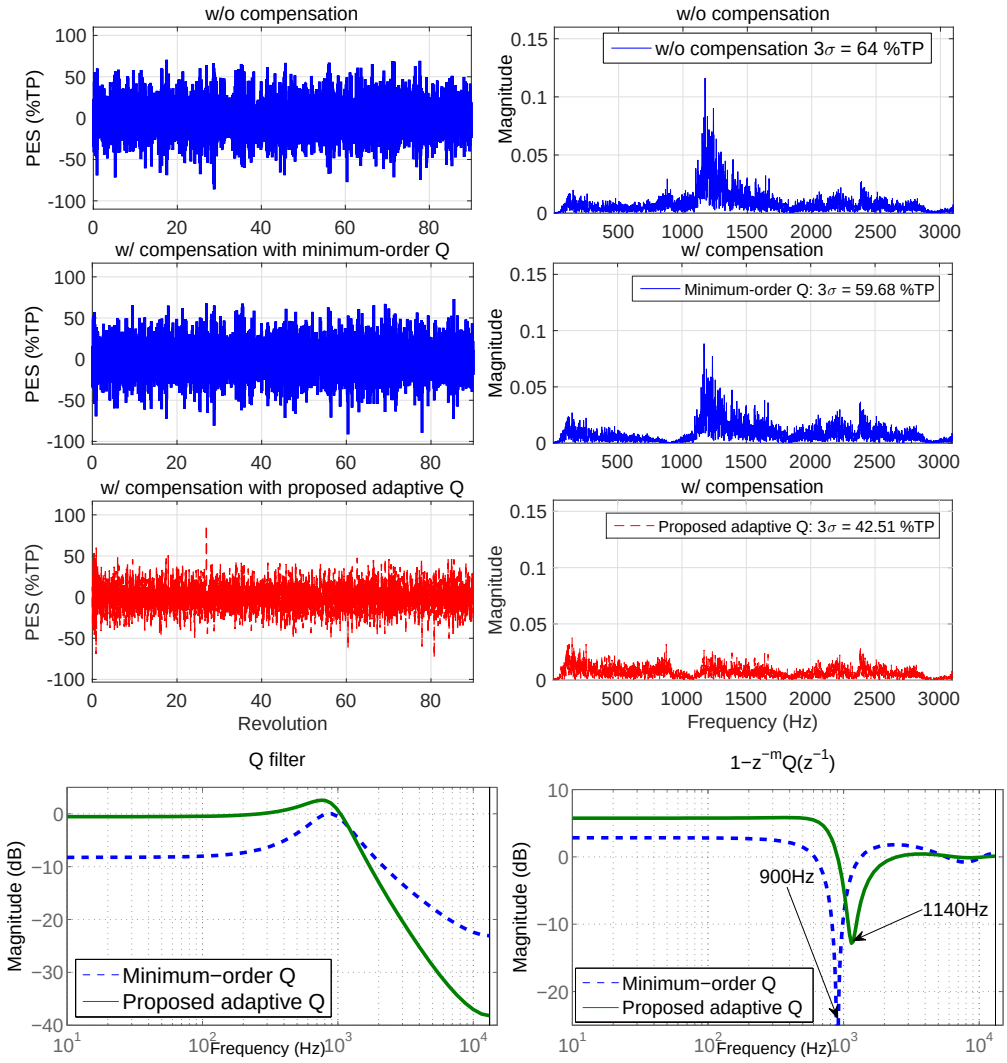

Figure 8: Performance robustness enhancement with the proposed controller

6 Conclusion

A direct adaptive control scheme based on DOB and flexible loop shaping was proposed. By introducing more freedom in the Q filter, the local loop shaping technique for narrow-band disturbance rejection has been extended to attenuate wide-spectrum disturbances. The proposed controller not only

reduced the "waterbed" effect but also enhanced the performance robustness with respect to uncertainties in the center frequencies. Simulation results on a HDD benchmark problem for audio vibration suppression verified the effectiveness of the proposed algorithm.

References

[1] R. Ehrlich and D. Curran, "Major hdd tmr sources and projected scaling with tpi," *Magnetics, IEEE Transactions on*, vol. 35, no. 2, pp. 885–891, 1999.

[2] L. Guo and Y.-J. Chen, "Disk flutter and its impact on hdd servo performance," *Magnetics, IEEE Transactions on*, vol. 37, no. 2, pp. 866–870, 2001.

[3] J. Q. Mou, L. Fukun, I. B. L. See, and W. Z. Lin, "Analysis of structurally transmitted vibration of hdd in notebook computer," *Magnetics, IEEE Transactions on*, vol. 49, no. 6, pp. 2818–2822, 2013.

[4] H. W. Bode, *Network analysis and feedback amplifier design*. D. van Nostrand New York, 1945.

[5] R. Ehrlich, J. Adler, and H. Hindi, "Rejecting oscillatory, non-synchronous mechanical disturbances in hard disk drives," *Magnetics, IEEE Transactions on*, vol. 37, no. 2, pp. 646–650, 2001.

[6] J. Zheng, G. Guo, Y. Wang, and W. E. Wong, "Optimal narrow-band disturbance filter for pzt-actuated head positioning control on a spin-stand," *Magnetics, IEEE Transactions on*, vol. 42, no. 11, pp. 3745–3751, 2006.

[7] I. D. Landau, A. Constantinescu, and D. Rey, "Adaptive narrow band disturbance rejection applied to an active suspension-an internal model principle approach," *Automatica*, vol. 41, no. 4, pp. 563–574, 2005.

[8] I. D. Landau, A. Constantinescu, and M. Alma, "Adaptive regulation - rejection of unknown multiple narrow band disturbances," in *Control and Automation, 2009. MED '09. 17th Mediterranean Conference on*, June 2009, pp. 1056–1065.

[9] T.-B. Airimitoaie and I. Landau, "Indirect adaptive attenuation of multiple narrow-band disturbances applied to active vibration control," *Control Systems Technology, IEEE Transactions on*, vol. 22, no. 2, pp. 761–769, 2014.

[10] E. Bertran and G. Montoro, "Adaptive suppression of narrow-band vibrations," in *Advanced Motion Control, 1998. AMC '98-Coimbra., 1998 5th International Workshop on*, June 1998, pp. 288–292.

[11] J. Levin and P. Ioannou, "Multirate adaptive notch filter with an adaptive bandwidth controller for disk drives," in *American Control Conference, 2008*, June 2008, pp. 4407–4412.

[12] Q. Zheng and M. Tomizuka, "A disturbance observer approach to detecting and rejecting narrow-band disturbances in hard disk drives," in *Advanced Motion Control, 2008. AMC '08. 10th IEEE International Workshop on*, March 2008, pp. 254–259.

[13] X. Chen and M. Tomizuka, "A minimum parameter adaptive approach for rejecting multiple narrow-band disturbances with application to hard disk drives," *Control Systems Technology, IEEE Transactions on*, vol. 20, no. 2, pp. 408–415, 2012.

[14] ——, "Overview and new results in disturbance observer based adaptive vibration rejection with application to advanced manufacturing," *International Journal of Adaptive Control and Signal Processing*, p. (to appear), 2015.

[15] B. Francis and W. Wonham, "The internal model principle of control theory," *Automatica*, vol. 12, no. 5, pp. 457–465, 1976.

[16] X. Chen, T. Jiang, and M. Tomizuka, "Pseudo Youla-Kucera parameterization with control of the waterbed effect for local loop shaping," *Automatica*, p. (to appear), 2015.

[17] X. Chen and M. Tomizuka, "Optimal decoupled disturbance observers for dual-input single-output systems," *Journal of Dynamic Systems, Measurement, and Control*, vol. 136, no. 5, pp. 1018–1031, 2014.

[18] L. Sun, X. Chen, and M. Tomizuka, "Adaptive suppression of high-frequency wide-spectrum vibrations with application to disk drive systems," in *2014 ASME Dynamic Systems and Control (DSC) Conference*, San Antonio, Texas, USA, October 2014.

[19] M. Tomizuka, T.-C. Tsao, and K.-K. Chew, "Analysis and synthesis of discrete-time repetitive controllers," *Journal of Dynamic Systems, Measurement, and Control*, vol. 111, no. 3, pp. 353–358, 1989.

[20] P. Regalia, "An improved lattice-based adaptive iir notch filter," *Signal Processing, IEEE Transactions on*, vol. 39, no. 9, pp. 2124–2128, 1991.

[21] L. Ljung, *System Identification: Theory for the User*, ser. Prentice-Hall Information and System Sciences Series. Pearson Education Canada, 1987.

[22] G. Li, "A stable and efficient adaptive notch filter for direct frequency estimation," *Signal Processing, IEEE Transactions on*, vol. 45, no. 8, pp. 2001–2009, 1997.

[23] D. Youla, J. J. Bongiorno, and H. Jabr, "Modern wiener–hopf design of optimal controllers part i: The single-input-output case," *Automatic Control, IEEE Transactions on*, vol. 21, no. 1, pp. 3–13, 1976.

[24] Y. Landau, *Adaptive Control: The Model Reference Approach*, ser. Control and System Theory. Taylor & Francis, 1979.

[25] V. Popov, *Hyperstability of control systems*, ser. Grundlehren der mathematischen Wissenschaften. Editura Academiei, 1973.

[26] M. Hirata, "Nss benchmark problem of hard disk drive system," 2007, http://mizugaki.iis.u-tokyo.ac.jp/nss/.